Original Research Article

Crash Analysis and Evaluation of the Security Road Blocker (SRB) Using Finite Element Method

Engin Metin Kaplan[1], Kemal Yaman[2*]

[1] Department of Mechanical Engineering, The Graduate School of Natural and Applied Sciences, Middle East Technical University (METU), 06800, Ankara, Turkey
[2] Defense Industries Research and Development Institute, Turkish Scientific and Technical Research Council, (TÜBİTAK-SAGE), 06261,Ankara, Turkey

Abstract

In this study, the crashworthiness of a medium heavy vehicle onto a designed security road blocker (SRB) as a vehicle barrier is studied numerically and compared with full-scale on-site crash test results in the literature. Structural integrity of the road blocker is studied by nonlinear dynamic methods under the loading conditions which are defined in the standards (ASTM F2656-07). Ls-Dyna ®software is used to solve the problem numerically. The penetration of the leading edge of the vehicle with respect to the attack face of the blocker is given both experimentally and numerically. Test and numerical results are compared. The comparison shows that; numerical results are in good agreement with the test results.

Key Words: Vehicle barrier, impact mechanics, finite element, crash analysis, security road blocker

*Corresponding author:
E-mail: kemal.yaman@tubitak.gov.tr

1. Introduction

Vehicle barriers are used as means of defense against any threat in open or closed areas to provide high security. Active barriers can be activated, either by personal, equipment, or both, to permit entry of a vehicle. Active barrier systems involve barricades, bollards, crash ribs, gates, and active tire shredders. On the other hand, passive barrier has no movable part. Passive barrier effectiveness is measured by its capability to absorb impact energy and transmit it to its foundation. Highway medians, bollards, tires, guardrails, ditches, and reinforced fences are example of passive barriers [1]. High security barrier systems may be kept in the ground or may be over the ground. Several design criteria must be considered in the design of a vehicle barrier. Furthermore, barrier is needed to provide qualifications that are defined in military standards. These standards [2] indicate the final position of the vehicle after the crash. Impact mechanic problems should be considered as shock problems rather than static problems since they take short time. In static states the energy applied to the structure is converted into strain energy. On the other hand, the collusion events do not provide enough time for strain to occur [3]. Deceleration at crash is seen to reach as much as 30 g. levels in some studies. Different materials can act in completely different in impact when compared to static loading conditions. Ductile materials like steel tend to become more brittle at high strain rates [4]. In addition to that, changes in the internal energy in the material can increase the temperature in impact problems. This must be evaluated, if it can cause difference in calculations. The calculations may be performed numerically and analytically.

The scope of this study is to design a security road blocker (SRB) with satisfactory performance under the effect of crash of a medium heavy truck. Solutions of this type of problems require the knowledge of impact mechanics and the implementation techniques of nonlinear dynamic finite element method. Then, by using this knowledge, appropriate element types, initial and boundary conditions can be determined. In this work, crash of a medium heavy vehicle onto a designed road blocker is studied numerically. There is very limited number of references in the literature about road blocker type vehicle barriers.

Several researchers have worked on crash of the vehicles to the barriers. Nelson and Hong studied inclined barrier impact of NASCAR series cars both experimentally and numerically. NASCAR, at the velocity of 135.6 mps, impacted to the barrier. Both NASCAR and barrier were modelled and investigated. Post processing was performed with explicit Ls-Dyna code. It is seen that the curved type barrier is more effective on deceleration of the cars than flat type barrier. Also, they compared the deceleration results of numerical model and test results. Deceleration levels of the numerical results and test results were in good agreement [5].

Road blockers used in anti-ram traffic barriers are widely employed in providing both security and positive control of normal traffic [6]. Originally designed and developed for embassies, bullion stores, military basis and other maximum security sites, road blockers are now popular at commercial buildings as they provide the ultimate in access control provision. Chirwa *et al* [6]. present results of a study carried out on the newly designed security road blocker that employed the upgraded specification PAS 68:2010. A baseline FE model of K12 SRB designed by Lace Control System was developed and analyzed in Ls-Dyna3D. As a baseline condition, the N2 type (7500 kg) commercial truck impacted the SRB perpendicularly head-on at a speed of 64 km/h as stipulated in PAS 68/2010 certification system. The maximum penetration of 246 mm could be achieved at the top edge of the middle plate of the SRB.

Hassan's study [7] is focused on impact of a car towards the two different barrier type's namely deformable and rigid barrier. They used explicit Ls-Dyna code to solve the

nonlinear dynamic equations. Stress results and wave propagation which was calculated in terms of stress, deformation pattern and plastic strain energy of the front rail of the vehicle was different in two different types of the solutions. On the other hand, it is seen that the final deformed shape of the vehicles is quite similar in numerical and experimental results.

Zaouk and Marzaugui compared the stress results and deformed shape results of the numerical and test results of the moveable deformable barrier's side impact effect study. Solution of the equation of motion was performed with explicit Ls-Dyna finite element code. They validated finite element results with the test results. Deformed shape of the car was captured by high speed camera in test. The deformation results of the test seem in a good agreement with the finite element solution. Acceleration data, which was validated with the test results. Besides that, they collected force data from a load cell which is located in the moveable barrier. The results of force data in test setup were quite similar with the numerical results [8].

Asadi *et al*. represented a new finite element simulation model for moving deformable barrier side impact analysis with explicit Ls-Dyna code. They also performed impact test to validate their result. A car on which a load cell was mounted hits two different barriers: flat pole and offset pole with a velocity of 35 km ph. The material properties of the finite element model were experimentally obtained with compression tests. Final comparison of the general results showed a strong correlation between test data and numeric results for both the Flat Wall and Offset Pole tests [9].

Ren and Vasenjak [10] studied on crash analysis of the road safety barrier. They developed a full-sale numerical model of the road safety barrier for use in crash simulations and to further compare it with the real crash test data. Finite element model of the car and barrier was prepared by beam and shell elements. Connections of the parts of the vehicle were

constraint with spot welds. Moreover, spring and damper elements were used to simplify calculations. The dynamic nonlinear elasto-plastic analysis was performed with the explicit finite element Ls-Dyna code. A car, weighing 900 kg has initial velocity of 100 km ph impacted to a barrier with an angle of 20° with respect to velocity vector. Car and barrier materials were bilinear elasto-plastic material model with kinematic hardening and failure criteria. They used effective plastic strain failure criteria and set the value to 0.28 which corresponds to 28% ductility. Automatic contact option was defined for parts. Friction coefficients for static and dynamic cases were taken as 0.1 and 0.05 respectively. According to EN 1317 standard, impact severity which is a measure of impact consequences for the vehicle is defined by acceleration severity index [11]. They compared the finite element results of acceleration severity index with the test results. Comparison of computational and experimental results proved the correctness of the computational model [11].

Borovinsek *et al*. developed Ren and Vasenjak's study. They prepared finite element models of a bus weighing 13-ton and a truck weighing 16-ton and impacted them to the barrier with an angle of 20° with respect to velocity vector. They also performed test setup of numerical model. Comparison of the computer simulation and a broad scale experiment demonstrated good correlation of computational and experimental results for both crash tests [12].

Yin *et al*. [13] made a security analyses about former girders, based in half vehicle model, analyzing the security of the front side member to reflect the vehicle's performance using Ls-Dyna. The Front side member have absorbed 50% of internal energy, the results proved that the former longitudinal structure's improvement is useful. And it will provide much help in improving the safety.

Chen *et al*. and TAY *et al*. were investigated the collision of anti-ram bollards security

barrier system for truck and pickup respectively [14, 15]. The medium-duty truck (Ford F800) is considered for crashing into a bollard at speed 50, 65, and 80 km/h. In this study, Ls-Dyna nonlinear finite element simulation of concrete filled steel tubular (CFT) bollards subjected to the impact of a medium-duty truck are carried out and validated against an actual truck collision test. Pickup (Toyota Hilux 4x4) results show that the numerical model is in good agreement with the test model.

Al-Thairy and Wang presented and validated a simplified numerical vehicle model that can be used to simulate the effects of vehicle (1994 model Chevrolet C2500 pick-up) frontal impact on steel columns by using the commercial finite element code ABAQUS/Explicit [16]. To validate the proposed numerical model, comparisons were made in terms of the load–deformation relationships of the vehicle and the axial load–critical impact velocity curves of the steel columns, between numerical simulation results using full-scale vehicle model and the simplified vehicle model. Very good agreement was achieved. National Crash Analysis Center performs crash tests to different vehicles [17]. They put several accelerometers on the vehicle and collect data from them. They also prepare finite element model and solve the differential equations by using explicit Ls-Dyna code. They used rigid barrier and deformable vehicle models. In this work, the vehicle crashed to the rigid barrier with a velocity of 35 km ph and an angle of 20° with respect to velocity vector.

The finite element model of the vehicles included shell, rib, solid, spring and damper elements. It is obvious that, velocity graphs of the vehicles demonstrate the reliability of the numerical studies. Acceleration data taken from the vehicle are generally close to numerical results. Besides that, energy balances which is obtained by numerical results also supports that results are reasonable.

2. Finite Element Analysis

2.1. System Constraints

During the design period of a SRB, system constraints are needed to be defined. System constraints are defined in standards, which are independent from the designers. There is a necessity to address a wide spectrum of a possible incident states such as credible threat vehicle types for the locale, impact energies and velocities of the various vehicle and different acceptable penetration limitations.

Test standards for security barriers are defined by ASTM. In that standard, the test vehicle was defined as a medium-sized vehicle weighing 6.8 tones. According to those weights different penetration limits are allowed for different crash velocities and kinetic energies.

Table 1. Penetration limitations for different vehicle velocities [18]

Required Velocities, [kmph][mph]	Maximum penetration Limits, [m][ft]
50 (30)	1 (3)
65 (40)	6 (20)
80 (50)	15 (50)

Required velocity and energy ranges are stated and scheduled in Table 1 and Table 2. Real vehicle velocities should be within permissible ranges stated to get the condition designation. The measured vehicle penetration to the SRB at the required crash velocity determines the dynamic penetration state for the condition designation.

Penetrations are referenced to the base of the forward corner of the passenger compartment on the small passenger car (C), the front leading lower edge of the pickup truck bed (P), the leading lower edge of the cargo bed on the medium duty truck (M) and the leading lower vertical edge of the cargo bed on the long heavy goods vehicle (H) [2]. Penetration limits are measured form the attack face of the barrier.

The vehicle that is used in the calculations is a Ford F800. The properties of the vehicle are appropriate for the design consideration as bolded in Table 2.

Table 2. Properties of different sized vehicles [18]

Test Vehicle [kg]	Minimum Test Velocity [km/h]	Permissible Speed Range [km/h]	Kinetic Energy [kj]	Condition Designation
Small Passenger Car (C) (1000)	65	60,1-75	179	C40
	80	75,1-90	271	C50
	100	90,1-above	424	C60
Pickup truck (P) (2300)	65	60,1-75	375	PU40
	80	75,1-90	568	PU50
	100	90,1-above	887	PU60
Medium Duty truck (M) (6800)	50	45-60	656	M30
	65	60,1-75	1110	M40
	80	75,1-above	1680	M50
Heavy Goods Vehicle (H) (29500)	50	45-60	2850	H30
	65	60,1-75	4910	H40
	80	75,1-above	7280	H50

2.2. Design Parameters

Once system constraints are defined, design parameters are to be studied for an active barrier. These parameters are height and width of the barrier, material selection, geometry of the ribs and alignment of the ribs. SRB systems can be considered in two different parts. Upper side of the barrier is the interface between vehicle impact face and the ground.
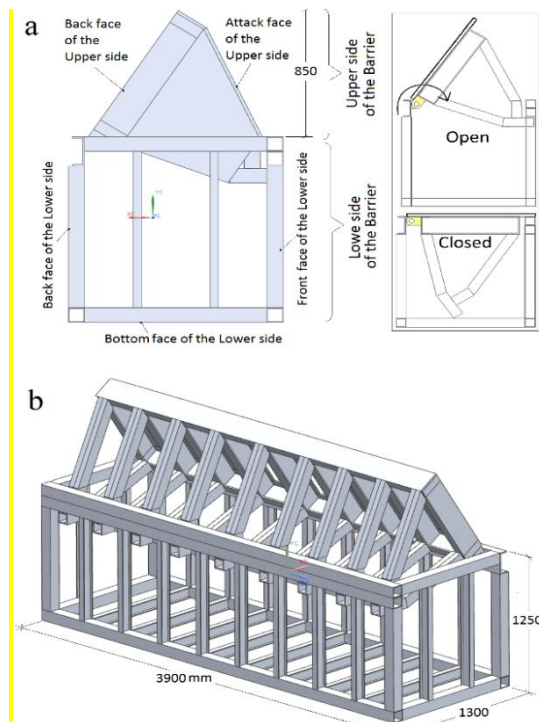

Figure 1. (a) Side view of the SRB CAD model and open-closed state of frame, (b) outer dimensions

It is located above the ground and can be penetrate underground. Lower side is located under the ground. It transfers the kinetic energy from the upper side of the barrier to the ground. The SRB example is given in Figure 1a. Typical systems are investigated. Most of the systems have at least 4 m. width and 1 m. height (The dimension which is above the ground). Also the embedded part(lower side) is at least 1 m. depth. Dimensions of the medium duty truck (Ford F800) are given in Table 3.

Table 3. Vehicle dimensions [19]

Height [m]	Width [m]	Length [m]	Weight [Tonne]
3.5	2.5	8.5	6.8

The dimensions for the perimeter of the barriers are given previously in Figure 1b. It can be understood that the dimensions of the barrier are adequate for the vehicle since width of the barrier is longer than the vehicle. Since the chassis parts are composed of welded joints, the material must have good weld ability properties. It also permits fabrication of elevated toughness welded joints even without further heat treatment. It is versatile regarding mechanical properties and corrosion-oxidation resistance. Secondly, toughness properties are significant in barrier design since barrier is induced impact effect during crash. It is stated that 304L series steels have excellent toughness, even down to cryogenic temperatures.

High-velocity collision (like a vehicle impact to the barrier) cannot be considered

as static effect. Materials behave as if they were more brittle in high velocity collusions [20]. Therefore, performance in cryogenic temperatures makes the AISI304L the most suitable material for a SRB. Moreover, joint materials must have high strength values since load is transmitted through them. Ph17-4 (precipitation hardening) steel is not only widely used, but also has high mechanical strength values. Shafts and bearings materials are selected as Ph 17-4 (H 900) stainless steel. Mechanical properties of the materials are given in Table 4.

Table 4. Mechanical properties of the SRB materials [21, 22]

Part	Material	E [GPa]	v	P [g/cm^3]	σ_{Yield} [MPa]
Ribs and Plates	AISI 304L	210	0,3	7,8	515
Joints	Ph 17-4 (H 900)	205	0,3	7,8	1345

2.3. Pre-Processing

In this study, the aim is to investigate the structural integrity of the SRB under an impulsive effect of the vehicle by explicit time integration method. Therefore, an equivalent numerical model is needed to be created.

2.3.1. Mathematical Model

All of the FEM model of vehicle components were downloaded from the internet [23]. Multiple parts of the vehicle body were modeled as plates. Therefore, plate-like structures are considered to simplify the solution. Four-node fully integrated elements were used due to its calculations are quicker than others. In addition to that, some chassis parts of the vehicle are modeled by beams (Hughes-Liu beam) [24].
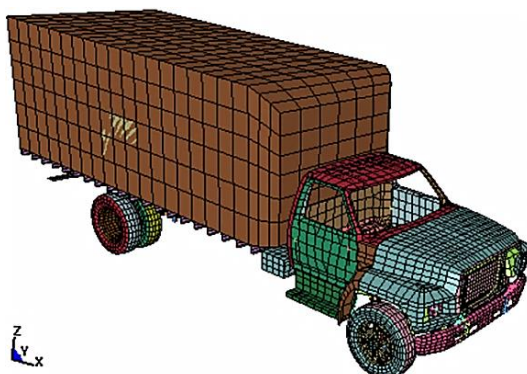

Figure 2. FEM of the vehicle [23]

The parts mesh model of the whole truck is given in Figure 2. Other structural solid type element is defined and calculated in the form of fully integrated eight-node hexahedral solid element. Welded connections of the different parts are connected each other with spot weld. In addition to the shear and normal forces for the failure of the welds are defined. In welded connections, all six DOFs of welded nodes are calculated equally. Tires were given as shell elements and connected to the vehicle with revolute joints. Pressure is applied to the interior element faces to simulate tire air pressure. It is not necessary to model detailed parts of the vehicle such as driver, engine and suspension system.

Mass equivalent models are built for engine, clutch and transmission. Point element mass model is performed for driver. Equivalent discrete spring and damper model were created for suspensions. Additional mass of the cargo and radiators were also modeled. Bolted connections in the vehicle were not modeled since it is computationally time consuming. Nodal rigid bodies are used instead of the bolts. Vehicle (frame, Bed, cabin, engine system, drive shaft, front suspension, front axle, rear suspension and axle, rear wheel), Parts are connected to each other with spot-weld. Frame is constructed with side and cross members, rear bumpers, suspension mounts, rear suspension brackets, vertical posts, stiffeners, tank brackets, front bumper supports and clutch bearings. Elements are created by three or four node shell elements. Frame cabin was generated with top cabin, bottom cabin, doors, wheel houses, hood, radiator grill and front bumper.

Parts are created by three or four node

shell elements. Parts are connected with spot-weld. A point element is constructed and located on the bottom cabin for driver.

2.3.2. Initial and Boundary Condition

Since the ground is supposed to be fixed, all displacement DOF of the ground and ground barrier housing model is constraint. Thus, SRB's degrees of freedom are constraint by positive contact of its ground housing model.
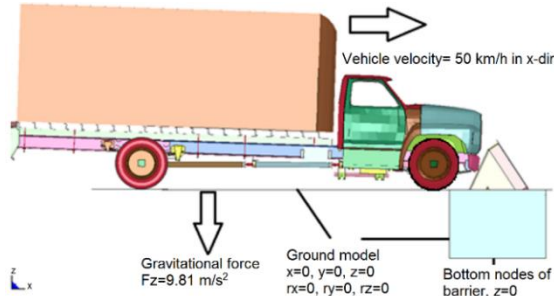

Figure 3. Initial and boundary conditions of the problem

SRB is connected to the ground from the bottom side with bolted joints. Instead of that, nodes at the bottom face of the SRBs' displacements are constraint in all directions. The vehicle is initially moved at 50 km ph in x direction through the barrier. Gravitational force is given for all parts in negative z direction as 9.81 m/s^2. Initial and boundary conditions are given in Figure 3.

2.3.3. Input Parameters

Mechanical material properties of the vehicle are given in Table 5. SRB parts yield strengths are scaled with a factor (0.85) due to indicate safety factor. The material properties of the SRB are already given in Table 4 previously.

Table 5. Mechanical properties of the vehicle parts used in analyses [23]

Vehicle Part	Behavior	E [GPa]	υ	ρ [g/cm^3]	σ_y [MPa]	ε_f [mm/mm]
Frame System	Elastoplastic	205	0,3	7,85	385	0,4
Bed System	Elastoplastic	205	0,3	7,85	155	0,3
Added Mas	Elastic	2	0,3	0,03	-	-
Cabin Sys.	Elastoplastic	205	0,3	7,85	155	0,4
Engine Sys.	Rigid	205	0,3	7,85	-	-
Suspension Sys.	Elastoplastic	205	0,3	7,85	700	0,1
Wheel Sys.	Elastic	205	0,3	7,85	-	-
Axle Sys.	Elastoplastic	205	0,3	7,85	385	0,4

Ground is modeled as rigid elements. Also, motions of the nodes are constrained in six directions. Because of no motion is calculated for the ground model, the input parameters are not significant. Linear Damper and nonlinear spring models are created to simulate suspension system with one dimensional element. The damping constant is specified as 1 [19]. Force vs. displacement curve of the nonlinear spring is given in Figure 4.
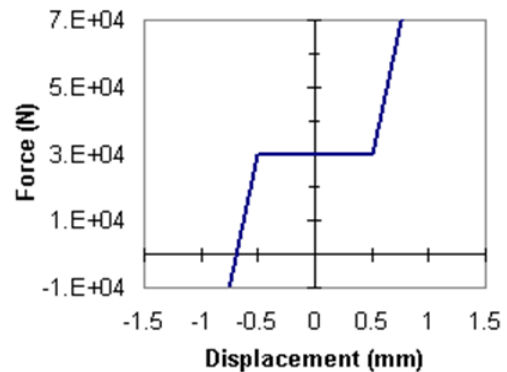

Figure 4. Force vs Displacement relationship of the nonlinear spring [25]

Weld spot failures when the constrained force between two nodes exceeds 50 kN [25]. Damping for the all steel materials is calculated as 0.02. Moreover, gravitational

force is accounted as 9.81 m/s^2.

2.3.4. Post-Processing

Hourglass energy, energy dissipation, damping energy and sliding energy are computed through the analysis and they are indicated to the energy balance. Moreover, displacement, velocity and acceleration are calculated for rigid and flexible bodies. In addition to that, principle strains, principle stresses, von Misses stresses and effective plastic strains are calculated for beam, shell and solid elements. Furthermore, kinetic energy, internal energy, sliding energy, hourglass energy and total energy are calculated. All results are calculated in one millisecond time intervals.

3. Crash Test On-Site Full-Scale Tests of SRB Barrier

Nowadays, each newly produced car must conform to the appropriate safety standards and norms. The most direct way to observe how a car behaves during a collision and to assess its crashworthiness is to perform a crash test [26].

The SRB barrier was performed for full-scale testing to better understand its strength and deformation characteristics by Crash Test Service (CTS) foundation in Munster/Germany [26]. Figure 5 Figa shows the truck and barrier profile view and Fig. 5b shows FEM model. The RB barrier is embedded toward 300 mm under the ground, and the two sides are backfilled using the same crushed rock to a thickness of 200 mm and topped by the 100 mm asphalt pavement. The length of the RB barrier is 3.9m same as the FEM model. The crash point is approximately at 780 mm from the truck approaching side, and the speed of the crash truck is 50 km/h which is currently the minimum design speed in the design specification of road barriers with respect to the ASTM F 2656 (M30) [2]. Due to the limitation of power of the pulling facility, a 6800 kg medium duty truck was used for collision tests. According to the ASTM F 2656 Standard design specifications of RB barrier, the maximum design impact energy is applied as 656 kJ.
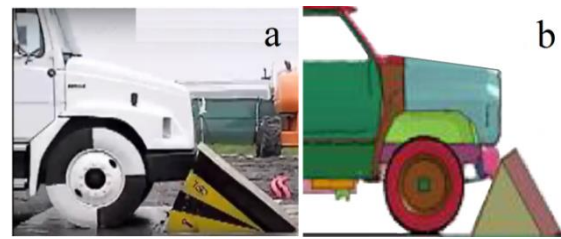

Figure 5. Profile view of Test [26] (a) Truck and barrier (b) Finite Element Model

4. Results and Discussions

The analysis is performed until the vehicle is spring backed from the SRB. Actually, velocity of the vehicle in x direction drops to zero at 0.135 seconds. But, it is important to observe the vehicle after this time. It is ensured that vehicle has consumed its kinetic energy at the end of the analysis. The SRB protects its structural integrity at the end of the numerical calculation. In addition to that maximum penetration of the leading lower edge of the vehicle to the attack face of the barrier is less than 1 m. in analysis. Thus, it can be said that SRB is successful according to designation ASTM F2656-07 standard numerically. The numerical results of initial and final displacement for upper and lower frame of SRB are given in Figure 6a and Figure 6b respectively.
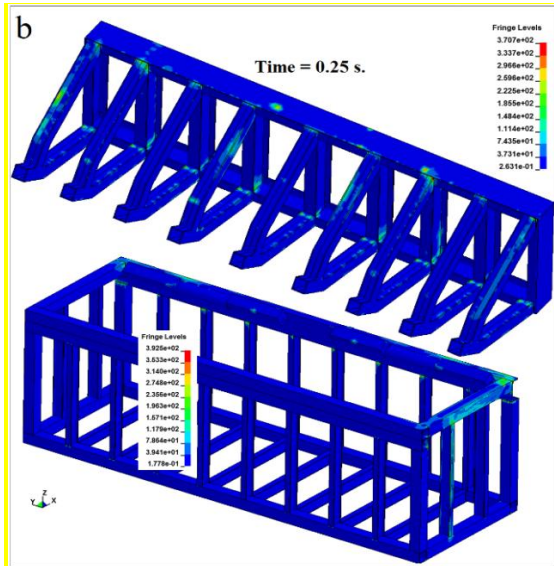

25
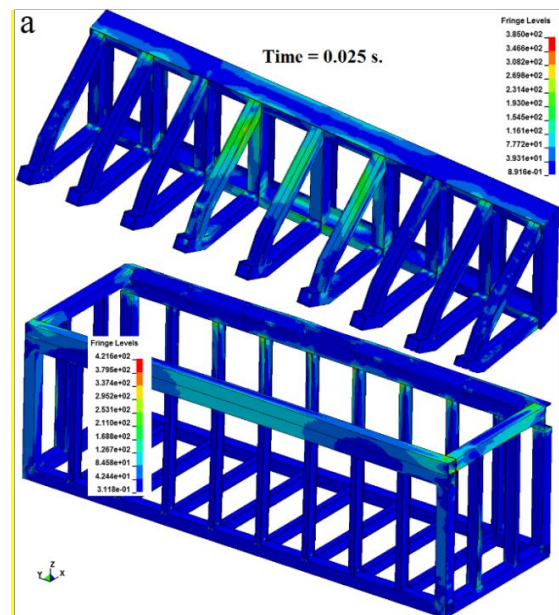
Figure 6. (a) FAE displacement results of upper and lower frame of SRB (a) initial, (t=0.025s) (b) final state of the crash (t=0.25s)

The deformed shape of the vehicle and the barrier is given in Figure2 7 by 0.25 s. time intervals. It can be understood that vehicle crashes and gets back.
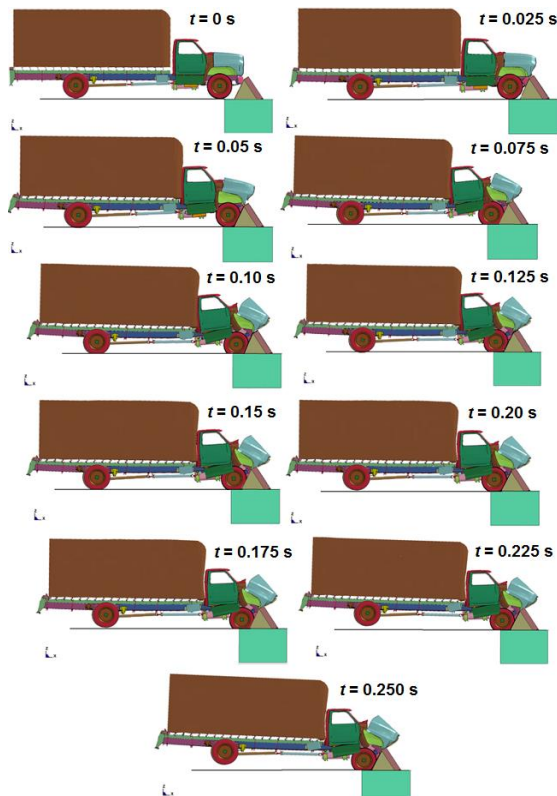

Figure 7. Deformed shape of the vehicle and the SRB in different time intervals Energy Results of the System

The energy balance during the analysis is given in Figure 8. It can be seen that total energy does not change during the

execution. In addition to that, kinetic energy reduces since velocity of the vehicle reduces. Internal energy increases since elastic and plastic strains occur.
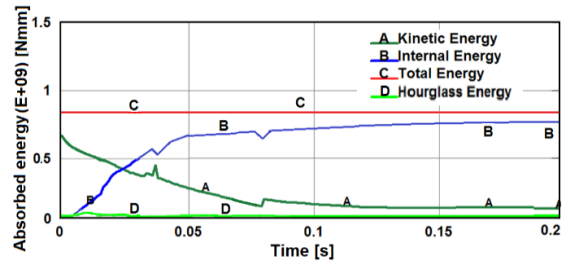

Figure 8. Energy balance versus time

Hourglass energy must be maximum %10 of the total energy during the analysis as it is mentioned before. The total energy and hourglass energy versus time domain is given in Figure 8. It can be seen that it is %1.75 of the total energy during the analysis. Suspension system is modelled by discrete springs and damper elements as it is mentioned before. The energy of the discrete elements is given in Figure 9. It can be seen that energy increases until the velocity of the vehicle is reduced to zero. After that point energy level decrease since the vehicle gets elevated after the crash.
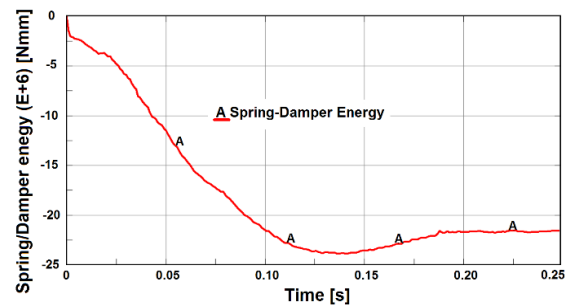

Figure 9. Variation of spring via damper energy

The damping energy of the system with respect to time domain is given in Figure 10. It can be seen that the slope of the graph decreases since energy of the system reduces.
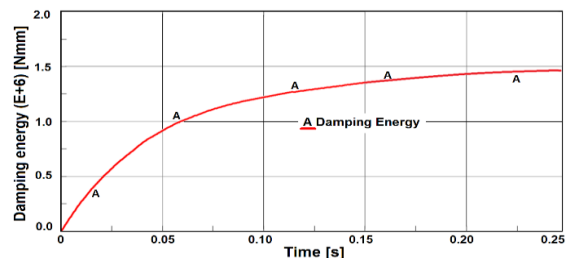

Figure 10. Damping energy vs. time

26

The penetration of the leading edge of the vehicle with respect to attack face of the SRB is given in Figure 11.
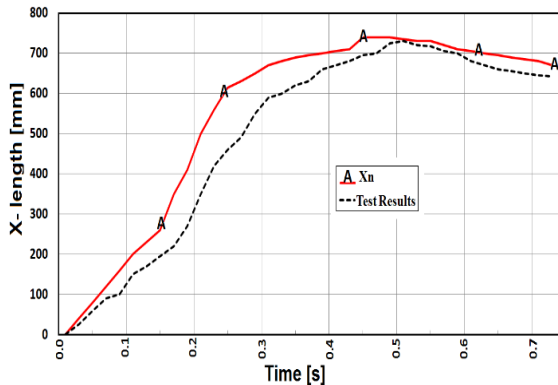

Figure 11. Displacement between vehicle leading edge with the attack face of the barrier vs. time

It can be seen that displacement increases up to 0.135 s. since vehicle does not lose its kinetic energy. Furthermore, it decreases after 0.175 s. since vehicle spring backs from the barrier. Penetration limit does not exceed 1000 mm as it can be seen in figure. According to the data obtained from on-site test, *x*-length penetration values are very close to the analysis values shown in Figure 11. The maximum penetration is observed as approximately 760 mm in the crash test.

Deceleration of the vehicle can be calculated by the help of the velocity graph. The total velocity drops to zero through that time interval gives the acceleration level. It is given in Figure 12.
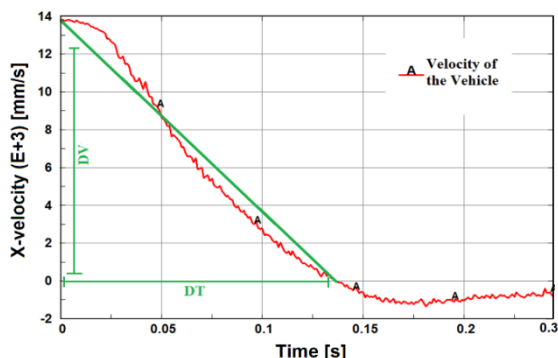

Figure 12. Deceleration calculation of the vehicle

The deceleration level (slope of the curve) is calculated about 10g. It is average value. Local high deceleration value can be higher than 10g. It can be said that different parts of the vehicle have alternating deceleration. Velocity graph,

shown in Figure 13 is taken from the added mass of the vehicle. In addition to that, the velocity drop graph taken from the different parts of the vehicle are also given in Figure 13.
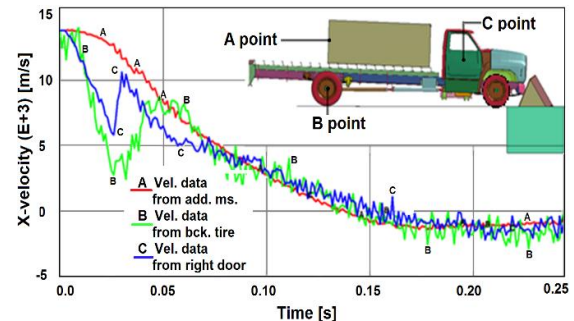

Figure 13. Velocity vs time graph taken from different parts of the vehicle

It can be said that the velocity drop initially occurs in the lower part of the vehicle. This is because of the height of the SRB. Attack face of the barrier firstly blocks the lower parts of the vehicle. It can be understood that, the curves move together after 0.1 seconds. It can be seen from the Figure 13 that, the space between bed and cabin gets minimized and moves back as the energy of the vehicle drops.

Total energy level is not changed during the analysis as shown in Fig. 8. Total energy is a composition of internal energy, kinetic energy, hourglass energy, spring-damper energy and damping energy. Internal energy of the system increases since the strain energy occurs in the parts as elastically and plastically. It is normal that kinetic energy drops since SRB blocks the motion of the vehicle. The sudden peaks and drops in the internal and kinetic energy may be cause of the element deletion of the parts. In addition to that, hourglass energy level is quite low according to total energy as it is shown in Fig. 8. Spring and damper energy increases in negative direction until impact effect is finished. The vehicle is elevated and probably the deflection of the damper and springs is reduced after that point. Therefore, the energy of the springs and dampers are reduced at the 0.15 seconds as it is shown in Figure 9. Later, equilibrium is broken and springs and dampers are

loaded again. Damping energy of the system has increasing value. But, the slope of the curve is decreased. This is because of the kinetic energy of the system is decreased.

In conclusion, SRB is investigated numerically with different aspects. It can be said that SRB is stable to the crash of the medium heavy vehicles as it is proven in this paper.

4.1. Penetration and structural Limit of the SRB

Penetration limit, which is defined as 1 m. in the standard, is seek according to variable vehicle velocity. According to analysis, at velocities which is greater than 59 km ph, SRB penetration limit exceeds 1m. Deformed shape is given in Figure 14 below.
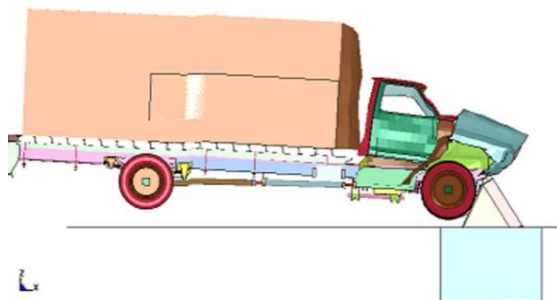

Figure 14. Penetration limit of the SRB

Structural Limit of the SRB is found. SRB cannot protect its structural integrity at velocity of 85 km ph. The crash view is given in Figure 15.
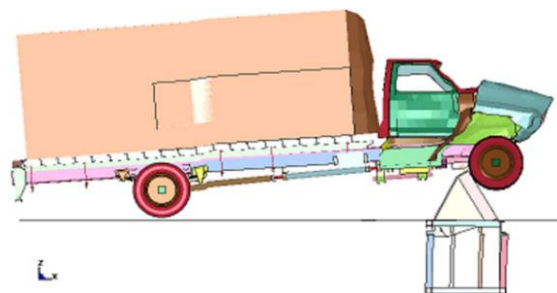

Figure 15. Structural integrity limit of the SRB

5. Conclusions

In this paper, computer analysis models were prepared for simulating the dynamic collision behaviors of both medium duty truck and security SRB barriers. The usefulness of these models was demonstrated via numerical examples by comparison with on-site full-scale experiment records (CTS/M30 Test No: 18250). This research made it possible to simulate the collision process, visualize the movement of the truck, and investigate the performances of SRB through the use of computers. Structural Limit of the SRB is found. According to the numerical results, the SRB cannot protect its structural integrity at velocity of 85 km ph. The penetration of the leading edge of the vehicle with respect to attack face of the blocker is given both experimentally and numerically in Figure 11. Numerical results are in good agreement with the test results. FE simulation was demonstrated to be a useful tool in crash analysis and decision-making process, and will be used in future research to investigate other variables important to designing the SRBs.

References

[1] Unified Facilities criteria (UFC), "Selection and application of vehicle barriers", USA, 1990.

[2] Designation F2656-07, "American Society of Test Materials (ASTM)", Standard Test Method for Vehicle Crash Testing of Perimeter Barriers.

[3] Goldsmith, W., "Impact Theory and Physical Behavior of Colliding Solids", Dover Publications, 2001.

[4] Poursartip, A., "Instrumented Impact Testing at High Velocities", Journal of Composites Technology and Research, vol. 15 issue 1, 1993.

[5] Nelson, E.A., Hong, L., "Curved barrier impact of a NASCAR series stock car", 8th International Ls-Dyna Users Conference, Crash Safety, Altair Engineering, M.I., U.S.A., 2004.

[6] Chirwa, E.C., Peng, Q., Lace, A., Matsika, E., Nowpada, S., "New generation of Security Road Blocker (SRB) Design and Its Performance Subjected to Commercial Vehicle Crash", The 8th International Forum of Automative Traffic Safety, Bolton Automative&Aerospace Research Group, University of Bolton, U.K., 2010.

[7] Hassan, J., "Interpretation of deformation pattern in automotive rails in frontal impact", 7th International Ls-Dyna Users Conference, Crash Safety, Scientific Labs and Proving Grounds DaimlerChrysler Corp., Detroit, USA, 2002.

[8] Zaouk, Abdullatif K., and Dhafer Marzougui. "Development and validation of a US side impact moveable deformable barrier FE model." 3rd European LS-DYNA Users Conference, Page. Vol. 14. 2001.

[9] Asadi, M., Tattersall, P., Walker, B., Shirvani, H., "Advanced Finite Element Model for AE-MDB Side Impact Barrier", 6th International Ls-Dyna Users Conference, USA, 2000.

[10] Ren, Z., Vesenjak, M., "Computational and experimental crash analysis of the road safety barrier", University of Maribor, Faculty of Mechanical Engineering, Slovenia, 2005.

[11] European Committee for Standardization, "European Standard EN 1317-1", EN 1317-2, Road Restraint Systems, 1998.

[12] Borovinsek, M., Vesenjak, M., Ulbin, M., Ren, Z., "Simulation of crash tests for high containment levels of road safety barriers", Eng. Failure Analysis, Vol.14(8):1711-1718, 2007.

[13] Yin, H.J., Jin, J., Yang, P.H., Pan, Y., Ma, S.K., "Simulation Analysis of Crash Tests for the Front Side Member in LS-DYNA", Adv. Materials Research, Vol.199/200:1200-1205, 2011.

[14] Chen, L., Xiao, G., Chunlin, L., Agrawal, A.K., "Test and numerical simulation of truck collision with anti-ram bollards" Int. J. of Impact Eng., 75:30-39, 20s.15.

[15] TAY, S.K., LIM, B., NG, S.H., "Crash Impact Modelling of Security Bollards", 12th. International Ls-Dyna Users Conf., 2012.

[16] Al-Thairy, H., Wang, Y.C., "Simplified FE vehicle model for assessing the vulnerability of axially compressed steel columns against vehicle frontal impact", J. of Const. Steel Research, 102:190-203, 2014.

[17] FHWA/NHTSA National Crash Analysis Center, "Finite Element Model of Chevy Silverado", The George Washington University, Version 2, 2007.

[18] Designation F2656-07, "American Society of Test Materials (ASTM)", Standard Test Method for Vehicle Crash Testing of Perimeter Barriers, 2007.

[19] Ford Company, "Ford F800 Truck Properties", Ford Truck Catalogues, USA, 2000.

[20] Sandvik Materials Technology Corporation, "Datasheet of SAF 3207 HD is a hyper-duplex (austenitic-ferritic) stainless steel", Seamless tube and pipe According to ASTM A789/A790, Mc Graw Hill, pp 37-38, Sweden, 2012.

[21] Material Property Database, "AISI 304L properties", Jahm Software, Inc., USA, 1998

[22] AK Steel Corporation, 17-4 PH Stainless Steel, "Product Data sheet", UNS S17400, 2007.

[23] NTRCI, http://thyme.ornl.gov/F800WebPage/ description/ description.html

[24] Yoo, Y. H., Yang, D. Y., "Finite element modeling of the high-velocity impact forging process by the explicit time integration method", J. Of Material Proc. Tech., Vol. 63(1):718-723, 1997.

[25] Marzougui, D., Mohan, P., Kan, S., "National transportation research center F800 Single Unit Truck FEM Model for Crash Simulations with Ls-Dyna", George Washington University, USA, 2007.

[26] Crash Test Service, Anti ramming Road Blocker, AUIA-313, ASTM F2656-07, M30, www. crashtest-service.com.